Acta Cryst E CRYSTALLOGRAPHIC COMMUNICATIONS

ISSN 2056-9890

Crystal structure and Hirshfeld surface analysis of 4′-chloro-5-oxo-*N*-phenyl-3-(thiophen-2-yl)-2,3,4,5-tetrahydro-[1,1′-biphenyl]-4-carboxamide monohydrate

Farid N. Naghiyev,[a] Victor N. Khrustalev,[b,c] Elena Yu. Nevskaya,[b] Mehmet Akkurt,[d] Jamshid M. Ashurov,[e] Hamouda Adam Hamouda[f]* and Ibrahim G. Mamedov[a]

[a]Faculty of Chemistry, Baku State University, Z. Khalilov str. 23, Az, 1148, Baku, Azerbaijan, [b]Peoples' Friendship University of Russia (RUDN University), Miklukho-Maklay St. 6, Moscow, 117198, Russian Federation, [c]N. D. Zelinsky Institute of Organic Chemistry RAS, Leninsky Prosp. 47, Moscow, 119991, Russian Federation, [d]Department of Physics, Faculty of Sciences, Erciyes University, 38039 Kayseri, Türkiye, [e]Institute of Bioorganic Chemistry, Academy of Sciences of Uzbekistan, M. Ulugbek Str.,83, Tashkent, 100125, Uzbekistan, and [f]Department of Chemistry, Faculty of Science, University of Kordofan, Sudan. *Correspondence e-mail: hamoudaadam84@gmail.com

Received 17 July 2026
Accepted 30 July 2026

Edited by X. Hao, Institute of Chemistry, Chinese Academy of Sciences

Keywords: crystal structure; face-to-face π–π interactions; thiophene ring; disorder; Hirshfeld surface analysis.

CCDC references: 2577790; 2577791

Supporting information: this article has supporting information at journals.iucr.org/e

The title molecule, $C_{23}H_{18}ClNO_2S\cdot H_2O$, has a stable conformation with *S*(5) and *S*(6) rings formed by intramolecular C—H···S and C—H···O hydrogen bonds. The water molecule and the carboxyl oxygen atom of the main molecule also make an O—H···O hydrogen bond. In the crystal, N—H···O, O—H···Cl, O—H···O and C—H···O hydrogen bonds connect molecules to form a three-dimensional network. The molecules are further connected by C—H···π interactions and face-to-face π–π interactions into layers parallel to the (001) plane.

1. Chemical context

Michael addition and aldol condensation reactions play a significant role in carbon–carbon bond formation, providing highly efficient and versatile strategies for the construction of complex molecular frameworks (Naghiyev *et al.*, 2023; Mamedov & Khalilov, 2025). These transformations enable the formation of new C—C bonds under relatively mild conditions, often with excellent regio- and stereoselectivity (Safarova *et al.*, 2023, 2024; Tüzün *et al.*, 2025). Owing to these advantages, Michael addition and aldol condensation reactions are widely employed in organic synthesis, particularly in the preparation of pharmaceuticals, natural products, and advanced functional materials (Naghiyev *et al.*, 2022, 2024; Karimli *et al.*, 2023). Among the products accessible through this synthetic approach, highly substituted cyclohexenone derivatives have attracted considerable attention owing to their structural diversity, widespread occurrence in both natural and synthetic compounds, and their utility as versatile intermediates in organic synthesis (Asgarova *et al.*, 2019; Abdel-Galil *et al.*, 2022). In addition to their synthetic importance, selected members of this class have been reported to exhibit a variety of biological activities, making cyclohexenone-based frameworks attractive targets in medicinal chemistry (Khan *et al.*, 2021; Shikhaliyev *et al.*, 2025). In particular, aryl-substituted cyclohexenone carboxamides represent valuable molecular scaffolds for the synthesis of structurally diverse compounds and continue to attract interest in synthetic and structural chemistry. The incorporation of aromatic, heteroaromatic, and amide functionalities into the

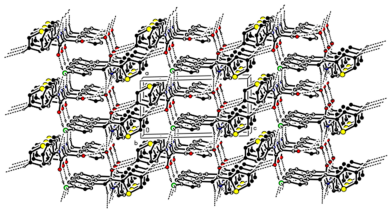

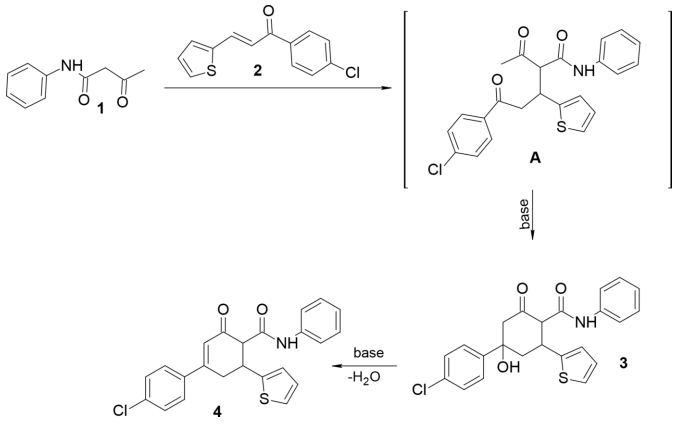

Figure 1
A reaction route for the formation of the title compound **4**.

cyclohexenone framework further expands the scope for structural diversification and detailed investigations of their molecular and crystal structures (Lakhrissi *et al.*, 2022; Nosova *et al.*, 2023). In this context, herein we report the crystal structure and Hirshfeld surface analysis of the title compound, $C_{23}H_{18}ClNO_2S{\cdot}H_2O$ (**4**), as part of our ongoing investigations (Askerov *et al.*, 2020; Naghiyev *et al.*, 2021; Khalilov *et al.*, 2011).

A reaction route for the formation of the title compound **4** is depicted in Fig. 1. The reaction is initiated by the Michael addition of the acetoacetamide **1** to the α,β-unsaturated chalcone **2**, leading to the formation of intermediate **A**. Under basic conditions, intermediate **A** undergoes intramolecular alkylation to form compound **3**, which then undergoes an intramolecular aldol condensation, resulting in the formation of the cyclohexane ring. Subsequent dehydration of this intermediate leads the corresponding cyclohexenone derivative **4**.

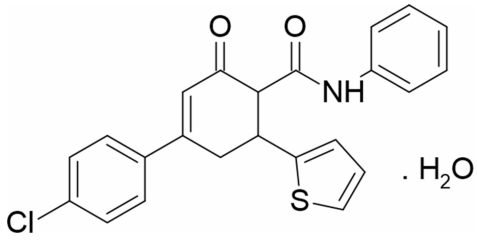

2. Structural commentary

The conformation of the title molecule is stable with the C—H···S and C—H···O intramolecular hydrogen bonding, forming *S*(5) and *S*(6) rings (Fig. 2, Table 1; Bernstein *et al.*, 1995). Additionally, an O*w*1—H*w*1*A*···O2 hydrogen bond exists between the water molecule and the main molecule's carboxyl oxygen atom. Each molecule contains two stereogenic (chiral) centres: in the arbitrarily chosen asymmetric unit, C2 and C3 have *S* and *R* configurations, respectively. The thiophene ring (S1/C13–C17) is disordered by a 180° rotation over two orientations around the C3—C14 bond in a 0.5:0.5 ratio. The cyclohexene ring (C1–C6) is puckered with Cremer & Pople (1975) puckering parameters Q_T = 0.4622 (9) Å, θ = 54.10 (11)° and φ = 112.74 (14)°. The r.m.s plane (r.m.s. deviation = 0.005 Å) of the cyclohexane ring (C1–C6) subtends dihedral angles of 73.1 (2), 70.72 (5) and 25.34 (4) °, respectively, with the thiophene (S1/C14–C17), phenyl (C8–C13) and chlorophenyl (C18–C23) rings. The thiophene ring subtends angles of 69.5 (2) and 86.6 (2)° with the phenyl and chlorophenyl rings, respectively. The angle between the phenyl and chlorophenyl rings is 84.58 (5)°. The bond lengths and angles in the title compound are in good agreement with those in the compounds discussed in the *Database survey* section.

Table 1
Hydrogen-bond geometry (Å, °).

*Cg*1 is the centroid of the major component of the disordered thiophene ring (S1/C14–C17).

D—H···*A*	*D*—H	H···*A*	*D*···*A*	*D*—H···*A*
N1—H1···O*w*1^{i}	0.881 (14)	1.953 (14)	2.8317 (10)	175.2 (12)
O*w*1—H*w*1*A*···O2	0.84 (2)	1.93 (2)	2.7681 (9)	171 (2)
O*w*1—H*w*1*B*···Cl1^{ii}	0.83 (2)	2.81 (2)	3.0653 (7)	100 (1)
O*w*1—H*w*1*B*···O1^{iii}	0.83 (2)	2.07 (2)	2.8908 (9)	172 (2)
C2—H2···S1	1.00	2.80	3.1912 (15)	104
C2—H2···O*w*1^{i}	1.00	2.50	3.3269 (10)	139
C9—H9···O2	0.95	2.32	2.9124 (11)	120
C16—H16···O2^{iv}	0.95	2.55	3.423 (6)	152
C17′—H17′···O2^{iv}	0.95	2.58	3.511 (5)	166
C11—H11···*Cg*1^{v}	0.95	2.91	3.801 (2)	158

Symmetry codes: (i) $x-1, y, z$; (ii) $-x+1, -y+2, -z+1$; (iii) $-x+1, -y+1, -z+1$; (iv) $-x+1, -y+1, -z+2$; (v) $x, y-1, z$.

3. Supramolecular features

In the crystal, molecules are linked to form a three-dimensional network *via* intermolecular N1—H1···O*w*1, O*w*1—H*w*1*B*···Cl1, O*w*1—H*w*1*B*···O1, C2—H2···O*w*1, C16—H16···O2 and C17′—H17′···O2 hydrogen bonds (Figs. 3 and 4, Table 1). In addition, C—H···π interactions and face-to-face π–π interactions [*Cg*5···*Cg*5($-x$, 2 − y, 1 − z) = 3.9020 (6) Å, slippage = 1.970 Å and *Cg*5···*Cg*5(1 − x, 2 − y,

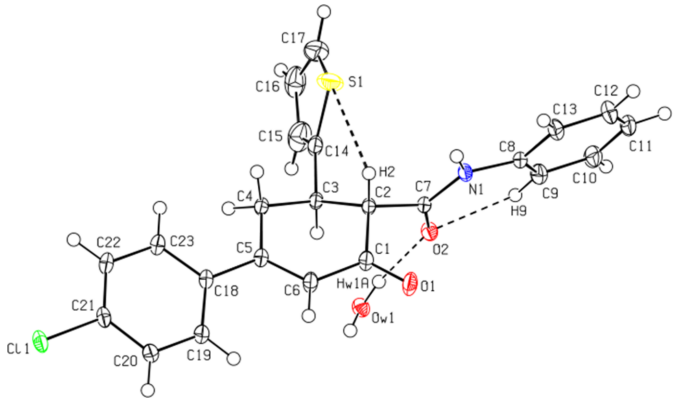

Figure 2
Molecular structure of the title compound, with atom labelling. Displacement ellipsoids are drawn at the 50% probability level. For clarity, only one component of the disordered thiophene ring is shown.

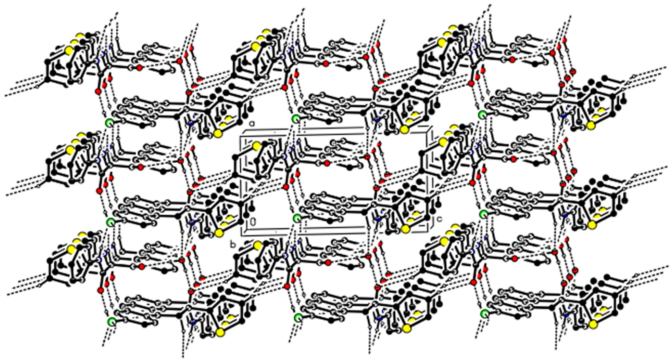

Figure 3
A view of the packing along the *b*-axis direction of the title compound with N—H···O, O—H···O, O—H···Cl and C—H···O hydrogen bonds shown as dashed lines. Hydrogen atoms that do not participate in hydrogen bonding are not displayed for clarity.

1 − *z*) = 3.5513 (6) Å, slippage = 0.158 Å; where *Cg*5 is the centroid of the C18–C23 ring of the chlorophenyl group] connect the molecules, forming layers parallel to the (001) plane (Figs. 5 and 6, Table 1).

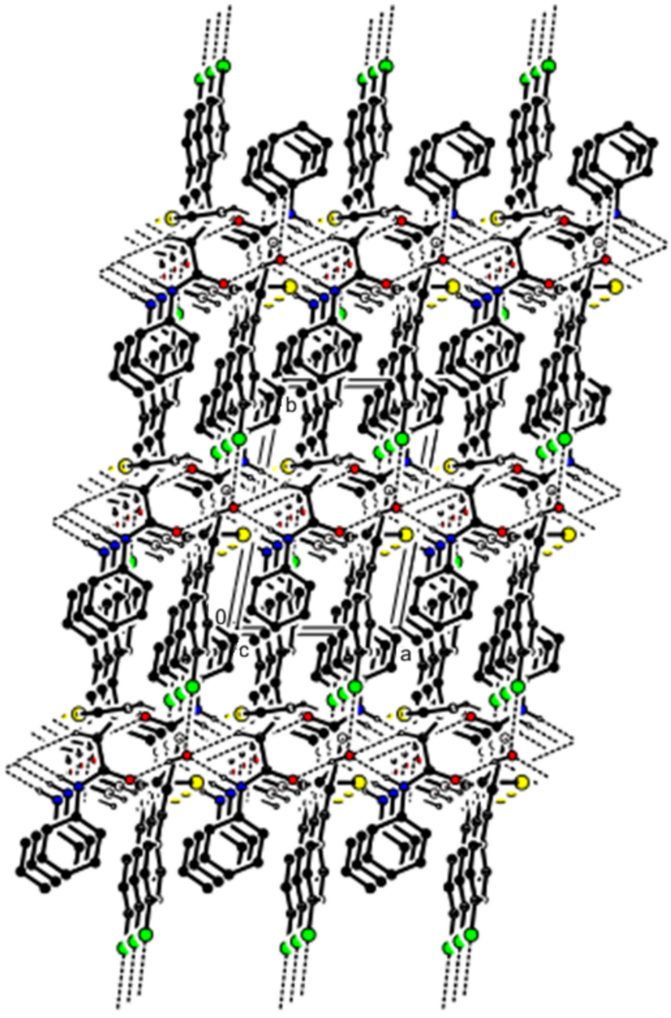

Figure 4
A view of the packing along the *c*-axis direction of the title compound with N—H···O, O—H···O, O—H···Cl and C—H···O hydrogen bonds shown as dashed lines.

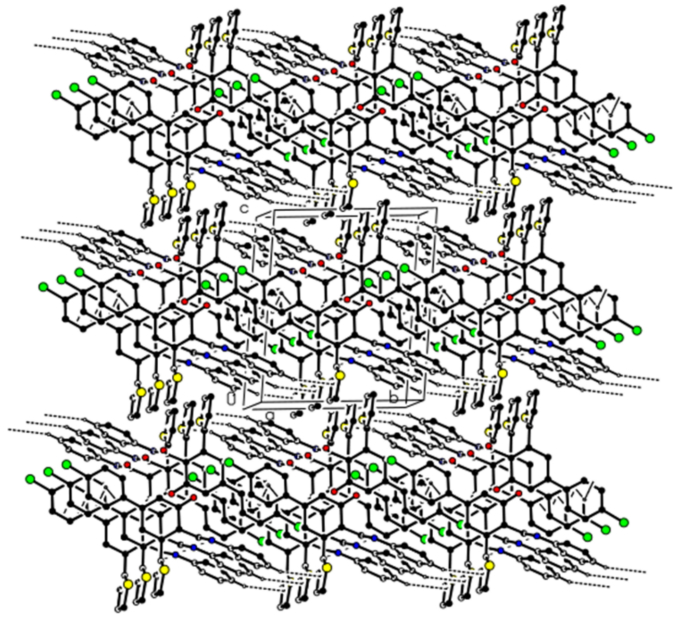

Figure 5
A view of the packing along the *a*-axis direction of the title compound with C—H···π and π–π interactions shown as dashed lines. Hydrogen atoms that do not engage in hydrogen bonding and water molecules are not shown for clarity.

4. Hirshfeld surface analysis

The Hirshfeld surfaces and two-dimensional fingerprint plots were produced using *Crystal Explorer 17.5* (Spackman *et al.*, 2021). Hirshfeld surfaces enable the presentation of intermolecular interactions by indicating short and long contacts, as well as the relative strength of the interactions, with different colors and intensities. Fig. 7 displays the title compound's three-dimensional Hirshfeld surface plotted over d_{norm} in the

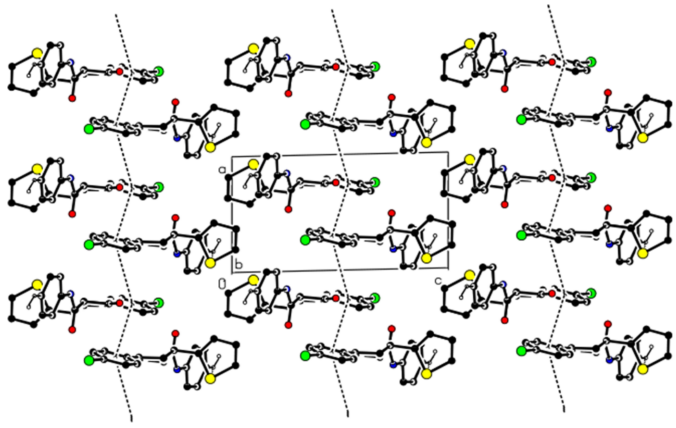

Figure 6
A view of the packing along the *b*-axis direction of the title compound with C—H···π and π–π interactions shown as dashed lines.

Table 2
Summary of short interatomic contacts (Å).

Contact	Distance	Symmetry operation
H23···C12	2.99	$x, 1 + y, z$
Cl1···H*w*1*B*	2.81	$1 - x, 2 - y, 1 - z$
H3···Cl1	2.83	$1 - x, 2 - y, 1 - z$
H4*A*···Cl1	2.88	$-x, 2 - y, 1 - z$
*H16′···C8	2.89	$-x, 1 - y, 2 - z$
*H16···H9	2.48	$1 - x, 1 - y, 2 - z$
O1···H*w*1*B*	2.07	$1 - x, 1 - y, 1 - z$
O2···H*w*1*A*	1.93	x, y, z
H19···O2	2.75	$1 - x, 1 - y, 1 - z$
H1···O*w*1	1.95	$-1 + x, y, z$

The prefix * indicates a disordered atom.

range −0.6301 to +1.6037 a.u. The red patch surrounding O1, O2, O*w*1 and Cl1 are caused by the N—H···O, O—H···Cl, O—H···O and C—H···O interactions (Table 1), which are crucial to the molecular packing of the title molecule.

Fig. 8*a* shows the overall two-dimensional fingerprint plot for the title compound, while Fig. 8*b–e* show those that are divided into H···H, C···H/H···C, O···H/H···O and Cl···H/H···Cl contacts. Tables 1 and 2 provide numerical information of the various contacts. The percentage contributions to the Hirshfeld surfaces from the different interatomic contacts are as follows: H···H (Fig. 8*b*; 43.2%), C···H/H···C (Fig. 8*c*; 22.2%), O···H/H···O (Fig. 8*d*; 12.5%) and Cl···H/H···Cl (Fig. 8*e*; 9.8%). The C···C (4.8%), S···H/H···S (3.2%), O···C/C···O (1.3%), N···H/H···N (1.2%), Cl···O/O···Cl (0.8%), Cl···C/C···Cl (0.7%) and O···O (0.3%) contacts are additional modest contributions to the Hirshfeld surface.

5. Database survey

A search of the Cambridge Structural Database (CSD, version 6.00, updated April 2025; Groom *et al.*, 2016) for the title compound revealed two compounds: 5-oxo-*N*-phenyl-3-(thiophen-2-yl)-2,3,4,5-tetrahydro-1,1′-biphenyl-4-carboxamide (CSD ref code AHEMIN: Aliyeva *et al.*, 2025) and dimethyl-4′-bromo-3-oxo-5-(thiophen-2-yl)-3,4,5,6-tetrahydro[1,1′-biphenyl]- 2,4-dicarboxylate (WOMWUU: Naghiyev *et al.*, 2024). AHEMIN and WOMWUU crystallize in the monoclinic *Cc* and $P2/_1c$ space groups, respectively.

The two molecules in the asymmetric unit of AHEMIN have different carboxamide moiety conformations. Intermolecular N—H···O hydrogen bonds in the crystal connect the molecules into chains that propagate parallel to the *c*-axis. While there are no π–π interactions between the molecules, there are weak C—H···π(ring) interactions. In WOMWUU, molecules form ribbons in the *b*-axis direction as a result of intermolecular C—H···S hydrogen bonds with $R_2^2(10)$ ring motifs. van der Waals forces between the ribbons maintain the cohesiveness of the crystal structure, whereas C—H···π interactions consolidate the ribbon structure. The thiophene group is disordered by a 180° rotation around one bond.

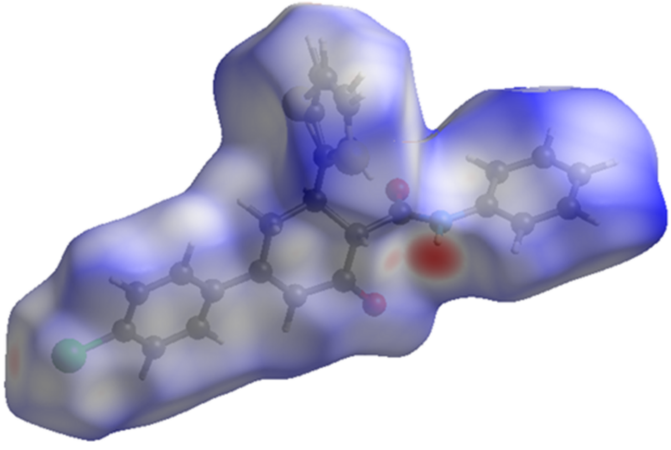

Figure 7
View of the three-dimensional Hirshfeld surface of the title compound plotted over d_{norm} in the range −0.6301 to +1.6037 a.u.

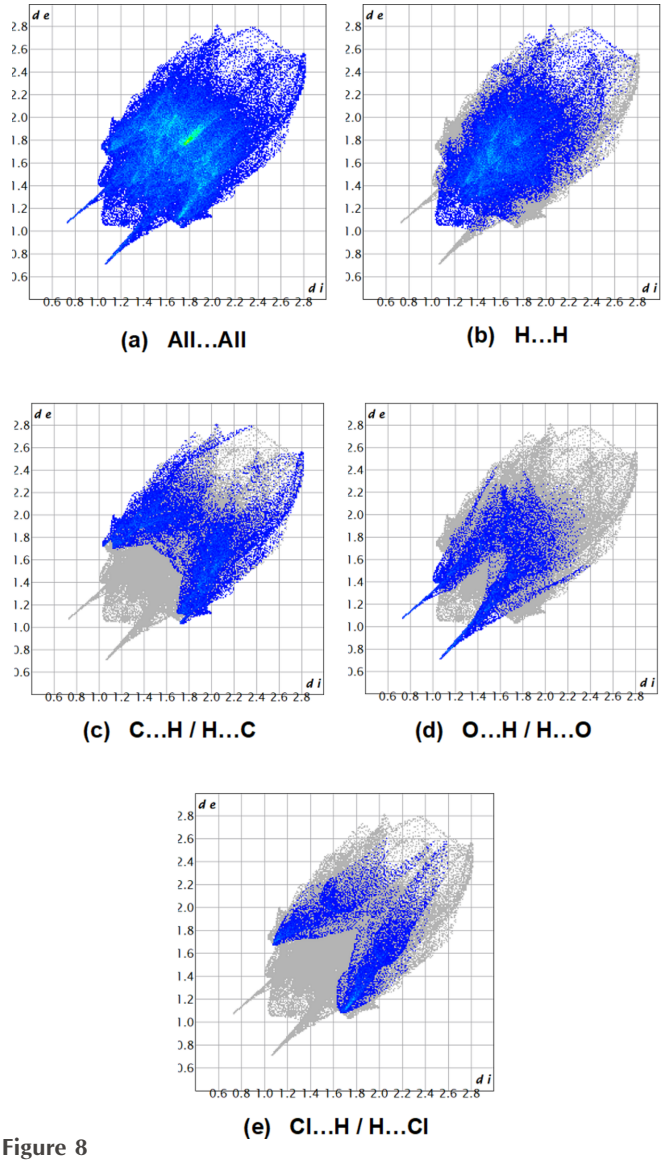

Figure 8
The full two-dimensional fingerprint plots for the title compound, showing (*a*) all interactions, and delineated into (*b*) H···H, (*c*) C···H/H···C, (*d*) O···H/H···O and (*e*) Cl···H/H···Cl interactions. The d_i and d_e values are the closest internal and external distances (in Å) from given points on the Hirshfeld surface.

Table 3
Experimental details.

Crystal data	
Chemical formula	$C_{23}H_{20}ClNO_3S$
M_r	425.91
Crystal system, space group	Triclinic, $P\overline{1}$
Temperature (K)	100
a, b, c (Å)	7.1577 (3), 11.1279 (4), 13.2067 (5)
α, β, γ (°)	85.412 (1), 87.973 (1), 79.348 (1)
V (Å^3)	1030.25 (7)
Z	2
Radiation type	Mo $K\alpha$
μ (mm^{-1})	0.31
Crystal size (mm)	0.24 × 0.22 × 0.13
Data collection	
Diffractometer	Bruker D8 QUEST PHOTON-III area detector
Absorption correction	Multi-scan (*SADABS*; Krause *et al.*, 2015).
T_{min}, T_{max}	0.707, 0.746
No. of measured, independent and observed [$I > 2\sigma(I)$] reflections	29949, 7470, 6538
R_{int}	0.026
(sin $\theta/\lambda)_{max}$ (Å^{-1})	0.758
Refinement	
$R[F^2 > 2\sigma(F^2)]$, $wR(F^2)$, S	0.033, 0.096, 1.04
No. of reflections	7470
No. of parameters	307
No. of restraints	171
H-atom treatment	H atoms treated by a mixture of independent and constrained refinement
$\Delta\rho_{max}$, $\Delta\rho_{min}$ (e Å^{-3})	0.47, −0.32

Computer programs: *APEX3* and *SAINT* (Bruker, 2018), *SHELXT* (Sheldrick, 2015*a*), *SHELXL* (Sheldrick, 2015*b*), *ORTEP-3 for Windows* (Farrugia, 2012) and *PLATON* (Spek, 2020).

6. Synthesis and crystallization

A solution of 0.443 g (0.0025 mol) acetoacetanilide and 0.623 g (0.0025 mol) 1-phenyl-3-(thiophen-2-yl)prop-2-en-1-one (5.10 mmol) in 30 ml ethanol (10 ml) was stirred for 1 h. After that, 3 drops of methylpiperazine were added to the solution and the mixture was then stirred for 3 h while the course of reaction was monitored by TLC. After the reaction completion, the solvent was removed under reduced pressure and the residue was recrystallized from an ethanol–water mixture (m.p. = 391 K, yield 73%).

^{1}H NMR (300 MHz, acetone-d_6, δ, ppm.): 2.22 and 2.72 (*d*-*d*, 2H, CH_2, $^2J_{H-H}$ = 16.2 Hz, $^3J_{H-H}$ = 8.3 Hz), 3.54 (*t*-*t*, 1H, CH, $^3J_{H-H}$ = 8.3 Hz, $^3J_{H-H}$ = 10.3 Hz), 3.78.15 (*d*, 1H, CH, $^3J_{H-H}$ = 10.3 Hz), 6.59–7.67 (*m*, 13H, arom. and ═CH), 9.56 (*s*, 1H, NH); ^{13}C NMR (75 MHz, acetone-d_6, δ, ppm.): 31.26 (CH), 44.45 (CH_2), 52.87 (CH), 119.08 ($CH_{arom.}$), 119.20 ($CH_{arom.}$), 120.35 ($C_{arom.}$), 123.17 (=CH), 127.00 ($CH_{arom.}$), 128.69 ($CH_{arom.}$), 129.47 ($CH_{arom.}$), 130.97 ($CH_{arom.}$), 132.13 ($C_{arom.}$), 131.13 ($CH_{arom.}$), 133.43 ($C_{arom.}$), 131.90 ($CH_{arom.}$), 138.36 ($C_{arom.}$), 147.33 ($C_{quat..}$), 167.27 (CO), 194.27 (CO).

7. Refinement

Crystal data, data collection and structure refinement details are summarized in Table 3. All C-bound hydrogen atoms were positioned geometrically (C—H = 0.95–1.00 Å) and refined using a riding model, with U_{iso}(H) = 1.2U_{eq}(C). The H atoms of the water molecule and NH group were located from difference-Fourier maps and refined isotopically with dependent isotropic thermal parameters with U_{iso}(H) = 1.2U_{eq}(N) and U_{iso}(H) = 1.5U_{eq}(O). The thiophene ring (S1/C13–C17) is disordered by a 180° rotation over two orientations around the C3—C14 bond in a 0.5:0.5 ratio. Using the FLAT command, both components of the disordered thiophene ring were restricted to the same plane. In addition, the DFIX command was used to restrain the S—C distances S1—C17, S1—C14, S1′—C17′ and S1′—C14 to fix their bond lengths to 1.72 Å. Furthermore, DELU, SIMU and ISOR commands were used in the refinement to restrain the thermal factors of the disordered C15 S1′, C16 C17′, C17 C16′ and C15′ S1components. Using the SADI command, the C—C lengths of the thiophene rings were pushed to be the same.

Acknowledgements

Authors' contributions are as follows. Conceptualization, FNN and IGM; methodology, FNN and IGM; investigation, JMA, MA and HAH; writing (original draft), MA and FNN; writing (review and editing of the manuscript), MA and FNN; visualization, MA, EYN and IGM; funding acquisition, VNK, HAH and FNN; resources, EYN, VNK, JMA and FNN; supervision, İGM and MA.

References

Abdel-Galil, E., Girges, M. M. & Said, G. E. (2022). *Russ. J. Gen. Chem.* **92**, 2169–2177.
Aliyeva, K. N., Hökelek, T., Khrustalev, V. N., Rzayev, R. M., Bhattarai, A., Maharramov, A. M. & Shikhaliyev, N. G. (2025). *Acta Cryst.* E**81**, 177–182.
Asgarova, A. R., Khalilov, A. N., Brito, I., Maharramov, A. M., Shikhaliyev, N. G., Cisterna, J., Cárdenas, A., Gurbanov, A. V., Zubkov, F. I. & Mahmudov, K. T. (2019). *Acta Cryst.* C**75**, 342–347.
Askerov, R. K., Maharramov, A. M., Khalilov, A. N., Akkurt, M., Akobirshoeva, A. A., Osmanov, V. K. & Borisov, A. V. (2020). *Acta Cryst.* E**76**, 1007–1011.
Bernstein, J., Davis, R. E., Shimoni, L. & Chang, N.-L. (1995). *Angew. Chem. Int. Ed. Engl.* **34**, 1555–1573.
Bruker (2018). *APEX3* and *SAINT*. Bruker AXS Inc., Madison, Wisconsin, USA.
Cremer, D. & Pople, J. A. (1975). *J. Am. Chem. Soc.* **97**, 1354–1358.
Farrugia, L. J. (2012). *J. Appl. Cryst.* **45**, 849–854.
Groom, C. R., Bruno, I. J., Lightfoot, M. P. & Ward, S. C. (2016). *Acta Cryst.* B**72**, 171–179.
Karimli, E. G., Khrustalev, V. N., Akkurt, M., Khalilov, A. N., Bhattarai, A., Aleskerova, A. N. & Mamedov, İ. G. (2023). *Acta Cryst.* E**79**, 777–781.
Khalilov, A. N., Abdelhamid, A. A., Gurbanov, A. V. & Ng, S. W. (2011). *Acta Cryst.* E**67**, o1146.
Khan, J., Ali, G., Rashid, U., Khan, R., Jan, M. S., Ullah, R., Ahmad, S., Abbasi, S. W., Khan Khalil, A. A. & Sewell, R. E. (2021). *Eur. J. Pharmacol.* **902**, 174091.
Krause, L., Herbst-Irmer, R., Sheldrick, G. M. & Stalke, D. (2015). *J. Appl. Cryst.* **48**, 3–10.
Lakhrissi, Y., Rbaa, M., Tuzun, B., Hichar, A., Anouar, H., Ounine, K., Almalki, F., Hadda, T. B., Zarrouk, A. & Lakhrissi, B. (2022). *J. Mol. Struct.* **1259**, 132683.

Mamedov, I. & Khalilov, A. (2025). *Baghdad Sci. J.* **22**, 2239–2245.
Naghiyev, F. N., Grishina, M. M., Khrustalev, V. N., Khalilov, A. N., Akkurt, M., Akobirshoeva, A. A. & Mamedov, İ. G. (2021). *Acta Cryst.* E**77**, 195–199.
Naghiyev, F. N., Khrustalev, V. N., Akkurt, M., Asadov, K. A., Bhattarai, A., Khalilov, A. N. & Mamedov, İ. G. (2024). *Acta Cryst.* E**80**, 446–451.
Naghiyev, F. N., Khrustalev, V. N., Akkurt, M., Khalilov, A. N., Bhattarai, A., Kerimli, F. S. & Mamedov, İ. G. (2023). *Acta Cryst.* E**79**, 494–498.
Naghiyev, F. N., Khrustalev, V. N., Dobrokhotova, E. V., Akkurt, M., Khalilov, A. N., Bhattarai, A. & Mamedov, İ. G. (2022). *Acta Cryst.* E**78**, 568–573.
Nosova, N. V., Sokolov, A. A., Gein, V. L., Dmitriev, M. V. & Mokrushin, I. G. (2023). *Russ. J. Gen. Chem.* **93**, 2742–2748.
Safarova, A. S., Khalilov, A. N., Akkurt, M., Brito, I., Bhattarai, A., Naghiyev, F. N. & Mamedov, I. G. (2023). *Acta Cryst.* E**79**, 1142–1146.
Safarova, A. S., Khalilov, A. N., Akkurt, M., Maharramov, A. M., Bhattarai, A., Naghiyev, F. N. & Mamedov, İ. G. (2024). *Acta Cryst.* E**80**, 191–195.
Sheldrick, G. M. (2015*a*). *Acta Cryst.* A**71**, 3–8.
Sheldrick, G. M. (2015*b*). *Acta Cryst.* C**71**, 3–8.
Shikhaliyev, N. G., Cisterna, J., Gajar, A. M., Niyazova, A. A., Khalilov, A. N., Khrustalev, V. N., Belay, A. N. & Maharramov, A. M. (2025). *Acta Cryst.* E**81**, 662–666.
Spackman, P. R., Turner, M. J., McKinnon, J. J., Wolff, S. K., Grimwood, D. J., Jayatilaka, D. & Spackman, M. A. (2021). *J. Appl. Cryst.* **54**, 1006–1011.
Spek, A. L. (2020). *Acta Cryst.* E**76**, 1–11.
Tüzün, B., Agbektas, T., Naghiyev, F. N., Tas, A., Zontul, C., Ozum, U., Khalilov, A. N., Silig, Y., Çakmak, N. K. & Mamedov, I. G. (2025). *Monatsh. Chem.* **156**, 667–688.

supporting information

Acta Cryst. (2026). E**82** [https://doi.org/10.1107/S2056989026007826]

Crystal structure and Hirshfeld surface analysis of 4′-chloro-5-oxo-*N*-phenyl-3-(thiophen-2-yl)-2,3,4,5-tetrahydro-[1,1′-biphenyl]-4-carboxamide monohydrate

Farid N. Naghiyev, Victor N. Khrustalev, Elena Yu. Nevskaya, Mehmet Akkurt, Jamshid M. Ashurov, Hamouda Adam Hamouda and İbrahim G. Mamedov

Computing details

4′-chloro-5-oxo-*N*-phenyl-3-(thiophen-2-yl)-2,3,4,5-tetrahydro-[1,1′-biphenyl]-4-carboxamide monohydrate

Crystal data

$C_{23}H_{20}ClNO_3S$
M_r = 425.91
Triclinic, $P\overline{1}$
a = 7.1577 (3) Å
b = 11.1279 (4) Å
c = 13.2067 (5) Å
α = 85.412 (1)°
β = 87.973 (1)°
γ = 79.348 (1)°
V = 1030.25 (7) Å^3
Z = 2
$F(000)$ = 444
D_x = 1.373 Mg m^{-3}
Mo $K\alpha$ radiation, λ = 0.71073 Å
Cell parameters from 9950 reflections
θ = 2.3–32.6°
μ = 0.31 mm^{-1}
T = 100 K
Prism, colourless
0.24 × 0.22 × 0.13 mm

Data collection

Bruker D8 QUEST PHOTON-III area detector diffractometer
Radiation source: fine-focus sealed X-ray tube
φ and ω scans
Absorption correction: multi-scan (SADABS; Krause *et al.*, 2015).
T_{min} = 0.707, T_{max} = 0.746
29949 measured reflections
7470 independent reflections
6538 reflections with $I > 2\sigma(I)$
R_{int} = 0.026
θ_{max} = 32.6°, θ_{min} = 2.3°
h = −10→10
k = −16→16
l = −19→19

Refinement

Refinement on F^2
Least-squares matrix: full
$R[F^2 > 2\sigma(F^2)]$ = 0.033
$wR(F^2)$ = 0.096
S = 1.04
7470 reflections
307 parameters
171 restraints
Primary atom site location: difference Fourier map
Secondary atom site location: difference Fourier map
Hydrogen site location: mixed
H atoms treated by a mixture of independent and constrained refinement
$w = 1/[\sigma^2(F_o^2) + (0.0492P)^2 + 0.2767P]$ where $P = (F_o^2 + 2F_c^2)/3$
$(\Delta/\sigma)_{max}$ = 0.001
$\Delta\rho_{max}$ = 0.47 e Å^{-3}
$\Delta\rho_{min}$ = −0.32 e Å^{-3}

Special details

Geometry. All esds (except the esd in the dihedral angle between two l.s. planes) are estimated using the full covariance matrix. The cell esds are taken into account individually in the estimation of esds in distances, angles and torsion angles; correlations between esds in cell parameters are only used when they are defined by crystal symmetry. An approximate (isotropic) treatment of cell esds is used for estimating esds involving l.s. planes.

Fractional atomic coordinates and isotropic or equivalent isotropic displacement parameters (Å²)

	x	*y*	*z*	U_{iso}*/U_{eq}	Occ. (<1)
C1	0.25524 (13)	0.54707 (8)	0.56920 (7)	0.01765 (15)	
C2	0.23078 (11)	0.53684 (7)	0.68443 (6)	0.01457 (14)	
H2	0.091669	0.556861	0.701114	0.017*	
C3	0.32834 (12)	0.62985 (7)	0.73273 (6)	0.01465 (14)	
H3	0.468240	0.607450	0.718973	0.018*	
C4	0.25951 (12)	0.75980 (7)	0.68385 (6)	0.01542 (14)	
H4A	0.126226	0.788477	0.705986	0.019*	
H4B	0.337635	0.815674	0.708601	0.019*	
C5	0.27020 (12)	0.76730 (7)	0.56990 (6)	0.01545 (14)	
C6	0.27143 (14)	0.66615 (8)	0.51952 (7)	0.02000 (16)	
H6	0.283576	0.673274	0.447529	0.024*	
C7	0.30438 (12)	0.40503 (7)	0.72605 (6)	0.01440 (14)	
C8	0.18480 (13)	0.21554 (7)	0.78940 (7)	0.01687 (15)	
C9	0.35133 (14)	0.14688 (8)	0.83063 (7)	0.02207 (17)	
H9	0.465042	0.179672	0.827866	0.026*	
C10	0.34922 (16)	0.02935 (9)	0.87605 (8)	0.02666 (19)	
H10	0.462878	−0.017716	0.903714	0.032*	
C11	0.18444 (17)	−0.02001 (9)	0.88158 (8)	0.0278 (2)	
H11	0.184360	−0.099511	0.913681	0.033*	
C12	0.02000 (17)	0.04840 (9)	0.83956 (9)	0.0293 (2)	
H12	−0.093377	0.015232	0.842451	0.035*	
C13	0.01940 (14)	0.16499 (9)	0.79328 (8)	0.02353 (18)	
H13	−0.093866	0.210660	0.764102	0.028*	
C14	0.29646 (15)	0.62858 (8)	0.84584 (7)	0.02117 (17)	
S1	0.07641 (17)	0.62692 (14)	0.90037 (9)	0.0457 (3)	0.5
C15	0.4188 (7)	0.6373 (4)	0.9170 (4)	0.0418 (9)	0.5
H15	0.548435	0.636045	0.898030	0.050*	0.5
C16	0.3628 (7)	0.6481 (6)	1.0190 (5)	0.0381 (10)	0.5
H16	0.433302	0.663471	1.074719	0.046*	0.5
C17	0.1850 (8)	0.6312 (7)	1.0167 (5)	0.0408 (12)	0.5
H17	0.115541	0.621279	1.078447	0.049*	0.5
S1′	0.46619 (13)	0.65996 (9)	0.92283 (8)	0.02844 (15)	0.5
C15′	0.1394 (4)	0.6163 (4)	0.9066 (3)	0.0273 (7)	0.5
H15′	0.033929	0.592377	0.877244	0.033*	0.5
C16′	0.1295 (7)	0.6379 (6)	1.0101 (5)	0.0316 (8)	0.5
H16′	0.024541	0.641524	1.056513	0.038*	0.5
C17′	0.3053 (6)	0.6519 (6)	1.0255 (4)	0.0311 (9)	0.5
H17′	0.344876	0.657661	1.092569	0.037*	0.5
C18	0.27163 (12)	0.88751 (7)	0.51432 (7)	0.01561 (14)	

C19	0.32883 (13)	0.89587 (8)	0.41174 (7)	0.01929 (16)
H19	0.374162	0.823119	0.378549	0.023*
C20	0.32002 (13)	1.00903 (8)	0.35821 (7)	0.02015 (16)
H20	0.358267	1.014137	0.288616	0.024*
C21	0.25466 (12)	1.11474 (7)	0.40751 (7)	0.01738 (15)
C22	0.20179 (13)	1.11022 (8)	0.50943 (7)	0.01900 (16)
H22	0.160041	1.183503	0.542488	0.023*
C23	0.21107 (13)	0.99627 (8)	0.56233 (7)	0.01810 (15)
H23	0.175709	0.992008	0.632360	0.022*
N1	0.16715 (10)	0.33768 (6)	0.74663 (6)	0.01635 (13)
H1	0.0502 (19)	0.3750 (12)	0.7331 (10)	0.020*
O1	0.25246 (12)	0.45808 (6)	0.51977 (5)	0.02515 (15)
O2	0.47568 (9)	0.36629 (6)	0.73864 (5)	0.01807 (12)
OW1	0.79944 (9)	0.46463 (6)	0.69319 (5)	0.01883 (12)
HW1A	0.697 (2)	0.4412 (14)	0.7113 (11)	0.028*
HW1B	0.787 (2)	0.4935 (14)	0.6336 (12)	0.028*
Cl1	0.24401 (3)	1.25584 (2)	0.33950 (2)	0.02180 (6)

Atomic displacement parameters (Å²)

	U^{11}	U^{22}	U^{33}	U^{12}	U^{13}	U^{23}
C1	0.0226 (4)	0.0124 (3)	0.0183 (4)	−0.0035 (3)	−0.0030 (3)	−0.0012 (3)
C2	0.0153 (3)	0.0109 (3)	0.0178 (3)	−0.0030 (2)	−0.0001 (3)	−0.0015 (3)
C3	0.0160 (3)	0.0113 (3)	0.0170 (3)	−0.0031 (2)	−0.0003 (3)	−0.0021 (3)
C4	0.0169 (3)	0.0116 (3)	0.0181 (3)	−0.0028 (3)	−0.0004 (3)	−0.0026 (3)
C5	0.0163 (3)	0.0116 (3)	0.0186 (4)	−0.0023 (3)	−0.0021 (3)	−0.0015 (3)
C6	0.0312 (4)	0.0126 (3)	0.0169 (4)	−0.0054 (3)	−0.0030 (3)	−0.0009 (3)
C7	0.0166 (3)	0.0115 (3)	0.0156 (3)	−0.0037 (3)	0.0013 (3)	−0.0022 (2)
C8	0.0216 (4)	0.0119 (3)	0.0175 (3)	−0.0046 (3)	0.0040 (3)	−0.0021 (3)
C9	0.0250 (4)	0.0155 (4)	0.0247 (4)	−0.0027 (3)	0.0007 (3)	0.0014 (3)
C10	0.0363 (5)	0.0165 (4)	0.0250 (4)	−0.0012 (4)	0.0012 (4)	0.0026 (3)
C11	0.0457 (6)	0.0146 (4)	0.0234 (4)	−0.0086 (4)	0.0073 (4)	−0.0004 (3)
C12	0.0372 (5)	0.0194 (4)	0.0342 (5)	−0.0146 (4)	0.0059 (4)	−0.0014 (4)
C13	0.0250 (4)	0.0171 (4)	0.0301 (5)	−0.0089 (3)	0.0025 (3)	−0.0010 (3)
C14	0.0335 (5)	0.0130 (3)	0.0177 (4)	−0.0056 (3)	−0.0003 (3)	−0.0021 (3)
S1	0.0633 (7)	0.0539 (6)	0.0305 (4)	−0.0366 (6)	0.0265 (5)	−0.0197 (4)
C15	0.056 (2)	0.0290 (16)	0.0385 (16)	−0.0025 (14)	−0.0092 (16)	−0.0007 (12)
C16	0.060 (3)	0.0246 (13)	0.0310 (17)	−0.008 (2)	−0.0159 (19)	0.0009 (11)
C17	0.058 (3)	0.0328 (15)	0.0297 (16)	−0.006 (2)	0.016 (2)	0.0002 (12)
S1′	0.0355 (4)	0.0243 (3)	0.0253 (3)	−0.0025 (2)	−0.0107 (3)	−0.0027 (2)
C15′	0.0265 (13)	0.0261 (10)	0.0308 (12)	−0.0103 (12)	−0.0016 (12)	0.0012 (8)
C16′	0.041 (2)	0.0289 (16)	0.0267 (13)	−0.0130 (17)	0.0071 (15)	−0.0024 (10)
C17′	0.040 (2)	0.0309 (13)	0.0195 (11)	−0.0014 (17)	−0.0011 (14)	0.0020 (9)
C18	0.0157 (3)	0.0114 (3)	0.0200 (4)	−0.0027 (3)	−0.0031 (3)	−0.0010 (3)
C19	0.0215 (4)	0.0133 (3)	0.0230 (4)	−0.0032 (3)	0.0020 (3)	−0.0021 (3)
C20	0.0217 (4)	0.0150 (3)	0.0236 (4)	−0.0044 (3)	0.0031 (3)	0.0001 (3)
C21	0.0141 (3)	0.0119 (3)	0.0264 (4)	−0.0038 (3)	−0.0032 (3)	0.0013 (3)
C22	0.0206 (4)	0.0115 (3)	0.0252 (4)	−0.0022 (3)	−0.0037 (3)	−0.0027 (3)

C23	0.0216 (4)	0.0127 (3)	0.0204 (4)	−0.0031 (3)	−0.0037 (3)	−0.0025 (3)
N1	0.0157 (3)	0.0119 (3)	0.0216 (3)	−0.0037 (2)	0.0011 (2)	−0.0003 (2)
O1	0.0433 (4)	0.0133 (3)	0.0204 (3)	−0.0078 (3)	−0.0033 (3)	−0.0034 (2)
O2	0.0153 (3)	0.0154 (3)	0.0232 (3)	−0.0030 (2)	−0.0006 (2)	0.0004 (2)
OW1	0.0164 (3)	0.0183 (3)	0.0222 (3)	−0.0051 (2)	−0.0008 (2)	0.0001 (2)
Cl1	0.01933 (10)	0.01286 (9)	0.03293 (12)	−0.00468 (7)	−0.00022 (8)	0.00400 (7)

Geometric parameters (Å, º)

C1—O1	1.2324 (10)	C14—C15′	1.379 (4)
C1—C6	1.4533 (12)	C14—S1	1.7112 (15)
C1—C2	1.5233 (12)	C14—S1′	1.7126 (13)
C2—C7	1.5287 (11)	S1—C17	1.753 (7)
C2—C3	1.5396 (11)	C15—C16	1.401 (7)
C2—H2	1.0000	C15—H15	0.9500
C3—C14	1.5025 (12)	C16—C17	1.323 (6)
C3—C4	1.5362 (11)	C16—H16	0.9500
C3—H3	1.0000	C17—H17	0.9500
C4—C5	1.5005 (12)	S1′—C17′	1.755 (5)
C4—H4A	0.9900	C15′—C16′	1.404 (8)
C4—H4B	0.9900	C15′—H15′	0.9500
C5—C6	1.3511 (11)	C16′—C17′	1.321 (5)
C5—C18	1.4751 (11)	C16′—H16′	0.9500
C6—H6	0.9500	C17′—H17′	0.9500
C7—O2	1.2346 (10)	C18—C23	1.4015 (12)
C7—N1	1.3494 (10)	C18—C19	1.4022 (13)
C8—C9	1.3942 (13)	C19—C20	1.3859 (12)
C8—C13	1.3993 (13)	C19—H19	0.9500
C8—N1	1.4146 (11)	C20—C21	1.3871 (12)
C9—C10	1.3971 (13)	C20—H20	0.9500
C9—H9	0.9500	C21—C22	1.3847 (13)
C10—C11	1.3874 (16)	C21—Cl1	1.7359 (9)
C10—H10	0.9500	C22—C23	1.3896 (12)
C11—C12	1.3858 (17)	C22—H22	0.9500
C11—H11	0.9500	C23—H23	0.9500
C12—C13	1.3886 (13)	N1—H1	0.880 (13)
C12—H12	0.9500	OW1—HW1A	0.845 (15)
C13—H13	0.9500	OW1—HW1B	0.827 (16)
C14—C15	1.328 (4)		

O1—C1—C6	121.35 (8)	C15—C14—C3	128.6 (2)
O1—C1—C2	120.62 (8)	C15′—C14—C3	131.85 (19)
C6—C1—C2	117.94 (7)	C15—C14—S1	109.6 (2)
C1—C2—C7	109.81 (6)	C3—C14—S1	121.63 (8)
C1—C2—C3	110.89 (7)	C15′—C14—S1′	107.14 (19)
C7—C2—C3	112.27 (7)	C3—C14—S1′	120.75 (8)
C1—C2—H2	107.9	C14—S1—C17	86.2 (2)
C7—C2—H2	107.9	C14—C15—C16	122.0 (4)

C3—C2—H2	107.9	C14—C15—H15	119.0
C14—C3—C4	109.73 (7)	C16—C15—H15	119.0
C14—C3—C2	112.58 (7)	C17—C16—C15	100.9 (5)
C4—C3—C2	110.46 (7)	C17—C16—H16	129.6
C14—C3—H3	108.0	C15—C16—H16	129.6
C4—C3—H3	108.0	C16—C17—S1	120.5 (5)
C2—C3—H3	108.0	C16—C17—H17	119.7
C5—C4—C3	113.34 (7)	S1—C17—H17	119.7
C5—C4—H4A	108.9	C14—S1′—C17′	88.12 (19)
C3—C4—H4A	108.9	C14—C15′—C16′	122.5 (3)
C5—C4—H4B	108.9	C14—C15′—H15′	118.8
C3—C4—H4B	108.9	C16′—C15′—H15′	118.8
H4A—C4—H4B	107.7	C17′—C16′—C15′	101.3 (5)
C6—C5—C18	120.87 (8)	C17′—C16′—H16′	129.4
C6—C5—C4	120.24 (7)	C15′—C16′—H16′	129.4
C18—C5—C4	118.84 (7)	C16′—C17′—S1′	120.4 (5)
C5—C6—C1	123.73 (8)	C16′—C17′—H17′	119.8
C5—C6—H6	118.1	S1′—C17′—H17′	119.8
C1—C6—H6	118.1	C23—C18—C19	118.45 (8)
O2—C7—N1	124.39 (8)	C23—C18—C5	120.60 (8)
O2—C7—C2	121.41 (7)	C19—C18—C5	120.93 (7)
N1—C7—C2	114.20 (7)	C20—C19—C18	120.78 (8)
C9—C8—C13	119.43 (8)	C20—C19—H19	119.6
C9—C8—N1	124.32 (8)	C18—C19—H19	119.6
C13—C8—N1	116.20 (8)	C19—C20—C21	119.17 (9)
C8—C9—C10	119.30 (9)	C19—C20—H20	120.4
C8—C9—H9	120.3	C21—C20—H20	120.4
C10—C9—H9	120.3	C22—C21—C20	121.71 (8)
C11—C10—C9	121.32 (10)	C22—C21—Cl1	119.59 (7)
C11—C10—H10	119.3	C20—C21—Cl1	118.69 (7)
C9—C10—H10	119.3	C21—C22—C23	118.61 (8)
C12—C11—C10	119.00 (9)	C21—C22—H22	120.7
C12—C11—H11	120.5	C23—C22—H22	120.7
C10—C11—H11	120.5	C22—C23—C18	121.24 (8)
C11—C12—C13	120.61 (10)	C22—C23—H23	119.4
C11—C12—H12	119.7	C18—C23—H23	119.4
C13—C12—H12	119.7	C7—N1—C8	128.77 (7)
C12—C13—C8	120.33 (10)	C7—N1—H1	116.0 (9)
C12—C13—H13	119.8	C8—N1—H1	115.2 (9)
C8—C13—H13	119.8	HW1A—OW1—HW1B	107.1 (14)

O1—C1—C2—C7	28.70 (11)	C4—C3—C14—S1′	−88.62 (9)
C6—C1—C2—C7	−154.57 (8)	C2—C3—C14—S1′	147.93 (7)
O1—C1—C2—C3	153.36 (8)	C15—C14—S1—C17	−2.6 (3)
C6—C1—C2—C3	−29.90 (11)	C3—C14—S1—C17	−178.3 (3)
C1—C2—C3—C14	176.17 (7)	C3—C14—C15—C16	172.9 (4)
C7—C2—C3—C14	−60.58 (9)	S1—C14—C15—C16	−2.4 (5)
C1—C2—C3—C4	53.12 (9)	C14—C15—C16—C17	7.4 (7)

C7—C2—C3—C4	176.37 (7)	C15—C16—C17—S1	−9.5 (7)
C14—C3—C4—C5	−174.95 (7)	C14—S1—C17—C16	7.9 (6)
C2—C3—C4—C5	−50.26 (9)	C15′—C14—S1′—C17′	0.2 (3)
C3—C4—C5—C6	22.67 (11)	C3—C14—S1′—C17′	174.9 (2)
C3—C4—C5—C18	−159.71 (7)	C3—C14—C15′—C16′	−169.1 (4)
C18—C5—C6—C1	−175.02 (8)	S1′—C14—C15′—C16′	4.8 (5)
C4—C5—C6—C1	2.54 (14)	C14—C15′—C16′—C17′	−8.1 (7)
O1—C1—C6—C5	178.22 (9)	C15′—C16′—C17′—S1′	8.0 (7)
C2—C1—C6—C5	1.51 (14)	C14—S1′—C17′—C16′	−5.4 (6)
C1—C2—C7—O2	80.63 (10)	C6—C5—C18—C23	159.74 (9)
C3—C2—C7—O2	−43.22 (11)	C4—C5—C18—C23	−17.86 (12)
C1—C2—C7—N1	−99.20 (8)	C6—C5—C18—C19	−18.63 (13)
C3—C2—C7—N1	136.95 (7)	C4—C5—C18—C19	163.77 (8)
C13—C8—C9—C10	−0.70 (14)	C23—C18—C19—C20	−2.01 (13)
N1—C8—C9—C10	176.37 (9)	C5—C18—C19—C20	176.40 (8)
C8—C9—C10—C11	−0.47 (15)	C18—C19—C20—C21	0.37 (13)
C9—C10—C11—C12	1.06 (16)	C19—C20—C21—C22	1.40 (13)
C10—C11—C12—C13	−0.49 (16)	C19—C20—C21—Cl1	−179.90 (7)
C11—C12—C13—C8	−0.67 (16)	C20—C21—C22—C23	−1.44 (13)
C9—C8—C13—C12	1.27 (14)	Cl1—C21—C22—C23	179.87 (7)
N1—C8—C13—C12	−176.04 (9)	C21—C22—C23—C18	−0.28 (13)
C4—C3—C14—C15	−96.7 (3)	C19—C18—C23—C22	1.97 (13)
C2—C3—C14—C15	139.8 (3)	C5—C18—C23—C22	−176.44 (8)
C4—C3—C14—C15′	84.6 (3)	O2—C7—N1—C8	3.06 (14)
C2—C3—C14—C15′	−38.9 (3)	C2—C7—N1—C8	−177.12 (8)
C4—C3—C14—S1	77.99 (10)	C9—C8—N1—C7	8.68 (14)
C2—C3—C14—S1	−45.46 (11)	C13—C8—N1—C7	−174.16 (9)

Hydrogen-bond geometry (Å, º)

*Cg*1 is the centroid of the major component of the disordered thiophene ring (S1/C14–C17).

D—H···*A*	*D*—H	H···*A*	*D*···*A*	*D*—H···*A*
N1—H1···O*w*1^{i}	0.881 (14)	1.953 (14)	2.8317 (10)	175.2 (12)
O*w*1—H*w*1*A*···O2	0.84 (2)	1.93 (2)	2.7681 (9)	171 (2)
O*w*1—H*w*1*B*···Cl1^{ii}	0.83 (2)	2.81 (2)	3.0653 (7)	100 (1)
O*w*1—H*w*1*B*···O1^{iii}	0.83 (2)	2.07 (2)	2.8908 (9)	172 (2)
C2—H2···S1	1.00	2.80	3.1912 (15)	104
C2—H2···O*w*1^{i}	1.00	2.50	3.3269 (10)	139
C9—H9···O2	0.95	2.32	2.9124 (11)	120
C16—H16···O2^{iv}	0.95	2.55	3.423 (6)	152
C17′—H17′···O2^{iv}	0.95	2.58	3.511 (5)	166
C11—H11···*Cg*1^{v}	0.95	2.91	3.801 (2)	158
C11—H11···*Cg*2^{v}	0.95	2.86	3.757 (2)	158

Symmetry codes: (i) *x*−1, *y*, *z*; (ii) −*x*+1, −*y*+2, −*z*+1; (iii) −*x*+1, −*y*+1, −*z*+1; (iv) −*x*+1, −*y*+1, −*z*+2; (v) *x*, *y*−1, *z*.